Ptychographic phase microscope based on high-speed modulation on the illumination beam

Yudong Yao
Suhas P. Veetil
Cheng Liu
JianQiang Zhu

Ptychographic phase microscope based on high-speed modulation on the illumination beam

Yudong Yao,[a,b,c] Suhas P. Veetil,[d] Cheng Liu,[a,b,*] and JianQiang Zhu[a,b]
[a]Shanghai Institute of Optics and Fine Mechanics, Key Laboratory of High Power Laser and Physics, Chinese Academy of Sciences, Shanghai, China
[b]National Laboratory on High Power Laser and Physics, Chinese Academy of Sciences, Shanghai, China
[c]University of Chinese Academy of Sciences, Beijing, China
[d]Higher Colleges of Technology, Department of Engineering Technology and Science, Fujairah, United Arab Emirates

Abstract. A type of ptychography-based phase microscope was developed by integrating a spatial light modulator (SLM) into a commercial wide-field light microscope. By displaying a moving pattern on the SLM to change the sample illumination and record the diffraction intensities formed, both the modulus and phase of the transmission function of the sample could be accurately reconstructed with formulas similar to those of common ptychography. Compared with other kinds of phase microscopes, the developed microscope has several advantages, including its simple structure, high immunity to coherent noise, and low requirement for quality optics. In addition, defects in the illumination beam are also removed from the reconstructed image. Further, this microscope's fast data acquisition ability makes it highly suitable for many applications where highly accurate quantitative phase imaging is important, such as in living cells or other fragile biological samples that cannot sustain continuous imaging over a long period of time. © *2017 Society of Photo-Optical Instrumentation Engineers (SPIE)*
[DOI: 10.1117/1.JBO.22.3.036010]

1 Introduction

Phase-contrast imaging techniques play a pivotal role in advancing optical microscopic imaging as they are essential for biological samples that do not contain large quantities of natural pigments; thus, making them phase objects rather than amplitude objects.[1] Staining and labeling techniques using fluorescent and other exogenous dyes have been adopted in several studies to obtain high-contrast images.[2,3] However, these methods often require manipulation and interruption of the cell, resulting in destruction of the normal structure of the cell. Phase microscopy is an alternative technique that can be used to obtain higher contrast from phase objects using only optical means. This technique has become an important tool in many research fields, including biomedicine, material science, chemistry, and crystallography.[4–6] Based on applied techniques, phase microscopy devices can be broadly divided into two categories. The first category is based on the Zernike phase contrast and differential intensity contrast (DIC) used to achieve a qualitative observation of the phase object. The second category is based on digital holographic microscopy (DHM) and the transport-of-intensity equation (TIE) used to achieve a quantitative phase measurement. Although the first category works with incoherent illumination and thus is convenient for most studies, the image obtained is not a direct phase distribution of the light field observed, hence it is not suitable for quantitative analysis. Further, this kind of microscope is critically dependent on the quality of its optical components.[7–9] The second category of phase microscopes can provide quantitative information on the phase distribution of the transmitted or reflected light field.

In DHM, the use of a reference beam makes the device complex and very sensitive to environmental disturbances. Speckle noise inevitably appears in most experiments because of the highly coherent illumination.[10] TIE-based microscopy is much simpler than DHM in setup and can use incoherent illumination to measure the wave front.[11] However, like DHM, TIE essentially measures the product of the illumination and the transmission function of the sample, thus the illumination errors cannot be excluded from the generated image. These limitations demand a kind of quantitative phase microscopy with a simple structure that is highly robust with regard to environmental disturbances. This type of microscopy would be beneficial in many interesting research applications.

Ptychography-based microscopy is a recently developed technique that can achieve a highly accurate quantitative phase measurement using a very simple setup and has been adopted in some important biological studies.[12–16] The most important advantage of ptychography is that the generated image is free from the illumination errors and aberrations of the illumination optics, which is not the case for other phase microscopes. However, in conventional ptychography, the sample is scanned via a mechanical translation stage to acquire the large amount of data that are necessary to achieve a high-quality reconstruction and large field of view (FOV). This process substantially slows down data acquisition. Thus, this form of ptychography is not suitable for imaging dynamic samples, such as fresh living cells or tissues (for example, early stage embryos of zebra fish). Fourier ptychographic microscopy (FPM) has been proposed to provide a wide FOV and high-resolution image of the sample, and this type of microscopy is implemented in the

Fourier frequency domain, unlike real-space ptychography.[17–23] Compared with FPM, the ptychography-based microscope has a much simpler structure, is easier to implement, and is compatible with most commercial microscopes, so it can provide a more flexible solution for phase-contrast microscopic imaging. However, a microscope based on mechanical scanning ptychography requires a time-consuming data acquisition process and substantial computation to obtain a high-quality reconstruction with position correction. Thus, any further improvements that can speedup data acquisition would make ptychography more relevant and applicable to address the current challenges of phase microscopy.

In this paper, a moving pattern displayed on the spatial light modulator (SLM) was used to form a fast-changing illumination on the sample to scan the illumination beam over the sample while the detector could record diffraction patterns. Formulas similar to those used in conventional ptychography were used to reconstruct the modulus and phase distributions of the sample, the transmission function of the SLM, and the incident light field simultaneously. To verify the feasibility of the proposed method, a series of experiments and detailed numerical simulations were carried out, and results showed that the SLM was successfully integrated into a commercial transmission wide-field microscope to form a practical ptychography-based phase microscope that can achieve high-quality quantitative phase imaging. Compared with other phase-contrast microscopy, such as DIC and DHM, the proposed method has a simple structure, highly coherent noise immunity, and lower quality requirement for the optics. In addition, this method removes defects in the illumination beam from the reconstructed image. Because the data acquisition time is fundamentally decreased in this method, it can be used in applications that require measuring living cells or other biological samples, where high imaging speed is always preferred and a large FOV is not necessary. Although a large FOV is always welcome, it is not required in many studies. For example, in several cases, such as observing fresh cultured cells, a high-resolution and fast imaging speed are expected and required, rather than a large FOV. The proposed technique successfully reduced the data acquisition time to 2.8 s, and this time can be further reduced with a charge-coupled device (CCD) camera with random access memory (RAM). These improvements could make the system capable of measuring large numbers of samples in the regime of visible light microscopy. More importantly, this method does not change the original structure of the microscope, other than replacing the halogen lamp with a laser diode and placing an SLM in front of the sample, which makes it easy to transform any commercial light microscope into a phase microscope.

2 Description of the Algorithm

In theory, the illumination on the SLM can be ideally regarded as a planar beam, and the transmission function of the SLM with moving patterns can be regarded as a known function. Then the imaging can be achieved with the common ptychography algorithm. However, in practice, these approximations seriously degrade the resolution and image quality because of some unexpected practical factors. To make the suggested method more practical, the sample, the moving pattern on the SLM, and the laser beam incident on the SLM all can be reconstructed simultaneously. This is convenient because distortion, optical aberrations, and inaccurate knowledge of the transmission function of the SLM no longer need to be considered.
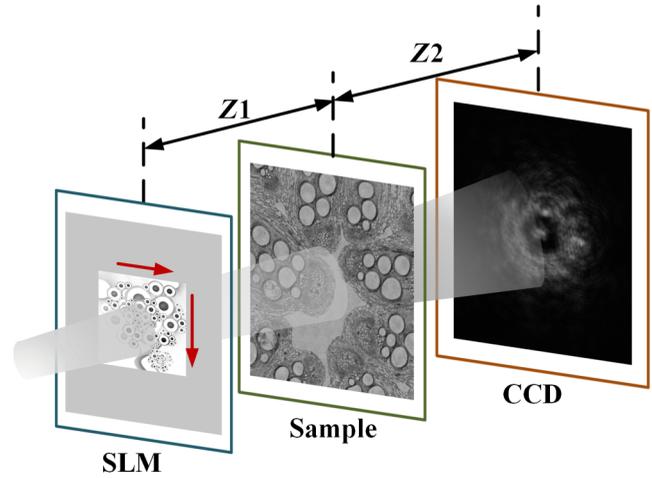

Fig. 1 Schematic of the proposed method to record diffraction patterns.

Figure 1 shows the schematic of the proposed method. A laser beam with a complex amplitude $E(\vec{r}_0)$ is incident on the SLM, and a preloaded picture on the SLM is moved in the x and y directions to form a series of complex transmission functions $T(\vec{r}_0 - \vec{R}_k)$, where $\vec{r}_0$ indicates the coordinate in the SLM plane and $\vec{R}_k$ corresponds to position of the moved picture. The sample with a transmission function $O(\vec{r})$ is located at a distance of z_1 behind the SLM, and a CCD camera is placed at a distance z_2 from the sample to record a set of diffraction pattern intensities $I_k(\vec{u})$ when the picture is displayed at different positions $\vec{R}_k$ on the SLM, where $\vec{r}$ and $\vec{u}$ are the coordinates of the sample and CCD plane, respectively.

The iterative reconstruction begins with a random initial guess for the transmission function $O_n(\vec{r})$ of the object, a uniform guess for the incident beam $E_n(\vec{r}_0)$ on the SLM, and a random initial guess of the transmission function $T_n(\vec{r}_0 - \vec{R}_k)$ of the SLM, where n stands for the iteration number. The diffraction patterns are addressed by a sequence k (k ranges from 1 to J). The reconstruction then iterates as follows:

(i) The illumination function on the sample is obtained by propagating the current guess of the exit wave $U_n(\vec{r}_0) = E_n(\vec{r}_0) \cdot T_n(\vec{r}_0 - \vec{R}_k)$ from the SLM as

$$P_{n,k}(\vec{r}) = \Im[E_n(\vec{r}_0) \cdot T_n(\vec{r}_0 - \vec{R}_k), z_1], \qquad (1)$$

where $\Im$ denotes the numerical wave propagation. The Fresnel propagation equation is used here because the distances z_1 and z_2 meet the near-field condition and the resolution obtained in the sample plane can be calculated to be higher than the pixel size of the CCD target. The exit function from the sample is then obtained by multiplying the current sample guess by the illumination function as follows:

$$V_{n,k}(\vec{r}) = O_n(\vec{r}) \cdot P_{n,k}(\vec{r}). \qquad (2)$$

(ii) The light field distribution in the detector plane is obtained as follows:

$$\psi_{n,k}(\vec{u}) = \Im[V_{n,k}(\vec{r}), z_2] = |\psi_{n,k}(\vec{u})|e^{j\theta_{n,k}(\vec{u})}, \qquad (3)$$

where $|\psi_{n,k}(\vec{u})|$ and $\theta_{n,k}(\vec{u})$ represent the amplitude and phase, respectively.

(iii) Like most phase retrieval algorithms,[24,25] the modulus of $\psi_{n,k}(\vec{u})$ is now replaced by the square root of the k'th diffraction pattern intensity $I_k(\vec{u})$,

$$\psi_{n,k}^{c}(\vec{u}) = \sqrt{I_k}e^{j\theta_{n,k}(\vec{u})}, \tag{4}$$

where the superscript c represents the corrected function.

(iv) An updated exit function is calculated by the inverse transform operation $\Im^{-1}$,

$$V_{n,k}^{c}(\vec{r}) = \Im^{-1}[\psi_{n,k}^{c}(\vec{u}), z_2]. \tag{5}$$

(v) The guessed sample transmittance function and the illumination function on the sample are updated using a Wigner filter-like equation,[14–15,20]

$$O_n^{c}(\vec{r})=O_n(\vec{r})$$
$$+\frac{|P_{n,k}(\vec{r})|}{|P_{n,k}(\vec{r})|_{\max}}\frac{P_{n,k}^{*}(\vec{r})}{[|P_{n,k}(\vec{r})|^2+\alpha]}(V_{n,k}^{c}-V_{n,k}), \tag{6}$$

$$P_{n,k}^{c}(\vec{r})=P_{n,k}(\vec{r})$$
$$+\frac{|O_n(\vec{r})|}{|O_n(\vec{r})|_{\max}}\frac{O_n^{*}(\vec{r})}{[|O_n(\vec{r})|^2+\beta]}(V_{n,k}^{c}-V_{n,k}), \tag{7}$$

where α and β are constant parameters to avoid zeroes in the denominators. The subscript max is the maximum value, and the superscript * signifies a conjugate function.

(vi) The updated illumination function $P_{n,k}^c$ is propagated back to the SLM plane

$$U_{n,k}^{c}(\vec{r}_0) = \Im^{-1}[P_{n,k}^{c}(\vec{r}), z_1]. \tag{8}$$

The incident beam and the transmission function of SLM are updated as follows:

$$E_n^{c}(\vec{r}_0) = E_n(\vec{r}_0)$$
$$+\frac{|T_n(\vec{r}_0 - \vec{R}_k)|}{|T_n(\vec{r}_0 - \vec{R}_k)|_{\max}}\frac{T_n^{*}(\vec{r}_0 - \vec{R}_k)}{[|T_n(\vec{r}_0 - \vec{R}_k)|^2 + \alpha]}$$
$$\times (U_{n,k}^{c} - U_{n,k}), \tag{9}$$

$$T_n^{c}(\vec{r}_0 - \vec{R}_k) = T_n(\vec{r}_0 - \vec{R}_k)$$
$$+\frac{|E_n(\vec{r}_0)|}{|E_n(\vec{r}_0)|_{\max}}\frac{E_n^{*}(\vec{r}_0)}{[|E_n(\vec{r}_0)|^2 + \beta]}$$
$$\times (U_{n,k}^{c} - U_{n,k}). \tag{10}$$

(vii) O_n^{c} and E_n^{c} are used as the improved object function and the incident beam on the SLM, respectively, and

$T_n^{c}(r_0 - R_k)$ is the improved transmission function of the SLM. Steps (i)–(vi) are repeated with the next diffraction pattern until all the diffraction patterns have been used.

(viii) Steps (i)–(vii) are repeated until the reconstruction error calculated according to Eq. (11) is sufficiently small.

$$\text{Err}_n = \frac{\sum_k \sum_{\vec{u}} |\sqrt{I_k} - |\psi_{n,k}||^2}{\sum_k \sum_{\vec{u}} I_k}. \tag{11}$$

Once the transmission function of the SLM and the illumination field are calibrated, $E_n(\vec{r}_0)$ and $T_n(\vec{r}_0 - \vec{R}_k)$ can be treated as known parameters for sample measurement. Hence, these two parameters do not need to be updated and only Eqs. (1)–(6) are used to retrieve the distribution of the sample.

3 Simulation Results

A numerical simulation was performed with the proposed algorithm to check its feasibility. A parallel laser beam with a wavelength of 632.8 nm was passed through a pinhole of 1.1 mm in diameter, which was used to control the size of the incident light beam on the SLM. The picture to be loaded on the SLM had the phase model shown in Fig. 2(a), which was normalized to a range from 0 to $\pi/2$ and had a size of 5.5 mm. The red square in Fig. 2(a) marks the region confining the illumination area on the SLM. The SLM used in the simulation had a pixel size of 27.5 μm. To simulate data acquisition, the picture was shifted in the x and y directions on the SLM with a step size of 0.275 mm to generate the shifted illuminations on the object. The test object is shown in Fig. 2, where Fig. 2(e) shows the modulus and Fig. 2(f) shows the phase. Diffraction patterns of 100 frames exiting from the object were recorded at 10×10 different picture positions on the SLM for reconstruction purposes. The distance between the SLM and the pinhole was maintained at 20 mm, and the distances between the SLM and the object and the object and the CCD were maintained at 200 and 50 mm, respectively. The CCD used in the simulation had 512×512 pixels with a pixel size of 5.5×5.5 μm^2.

With the algorithm described above, the object function was iteratively reconstructed using 100 frames of the diffraction patterns recorded. The reconstructed modulus and phase images are shown in Figs. 2(g) and 2(h). No noticeable difference was found when comparing them with the original images as shown in Figs. 2(e) and 2(f). The transmission distribution of the SLM could also be obtained as shown in Fig. 2(b), and the amplitude and phase of the incident beam on the SLM were reconstructed as shown in Figs. 2(c) and 2(d).

4 Experiment

The feasibility of the suggested method was also checked experimentally by integrating an SLM into a commercial optical microscope. As shown in Fig. 3, the main part of the system was an MI12 transmission wide-field microscope, and the light source was replaced by a He–Ne laser with a wavelength of 632.8 nm. An SLM loaded with a pattern was placed 35 mm in front of the sample. A nearly plane wave with a diameter of ~1 mm, together with the moving pattern on the SLM, generated a transverse scanning illumination on the sample. During
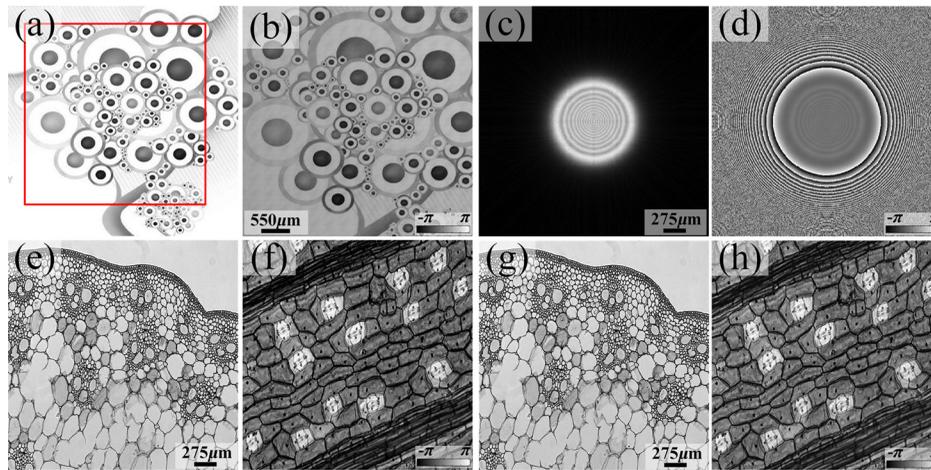
Fig. 2 (a) Pattern loaded on the SLM (the red square indicates the illuminated section on the SLM); (b) reconstructed phase distribution of the SLM; reconstructed (c) amplitude and (d) phase of the incident beam on the SLM; (e) amplitude and (f) phase of the original object; reconstructed (g) amplitude and (h) phase of the object.

data acquisition, the picture displayed in the SLM was shifted in the *x* and *y* directions to 100 different positions with a step size of 0.2368 mm, and the diffraction patterns were recorded at each position using a CCD camera (AVT Pike 421B). The CCD camera was attached to the camera port of a standard microscope by an extension tube and was placed 40 mm away from the imaging plane. The SLM used in this experiment was an electrically addressed SLM (Type GCI-77, China Daheng Optics), which had a fill factor of 68%. With a pixel size of $6.4 \times 6.4\ \mu m^2$, the diffraction angle of the first order of diffraction was ~5.6 deg. Because the distance between the SLM and the object was 35 mm and the diameter of the diffraction beam was ~1 mm, only the zeroth-order beam was used for imaging. All the other diffracted beams were far beyond the FOV of the objective lens and have no influence on the experimental results. A slice of pumpkin stem was used as the sample, and a 10× objective lens with numerical aperture (NA) of 0.25 was used. The reconstructed amplitude and phase of the sample shown in Figs. 4(a) and 4(b), respectively, were generated by 100 iterative computations, and the reconstruction results were very clear. In addition, both the complex amplitude of the transmission distribution of the SLM and the incident beam on the SLM were

obtained by the proposed method, as shown in Figs. 4(c)–4(f). Remarkably, the reconstructed results of the SLM show some amplitude modulation around the edges of the circles. The SLM adopted in this experiment works as a pure phase modulator when all technical requirements on both the wavelength and the polarization of the illuminating light are strictly met. However, in practice, the cross talk between the phase retardation and the energy absorption always takes place because of some unexpected factors.

The transmission function of SLM and the complex distribution of the incident laser beam can be premeasured; thus, both of them can be regarded as known parameters. The complex amplitude of the sample can be reconstructed by using a lower number of diffraction patterns in comparison with standard PIE, and 5×5 diffraction patterns are generally enough to obtain satisfying results with the proposed method. Figures 5(a) and 5(b) show the measurement results of a slice of corn seed with prior knowledge of the SLM and incident beam. Both the resolution and FOV of this microscopy system were determined by the objective lens, which was used to collect the diffractive data. For a 10× objective lens with an NA of 0.25, the theoretical resolution is defined as λ/NA, which is the smallest periodicity
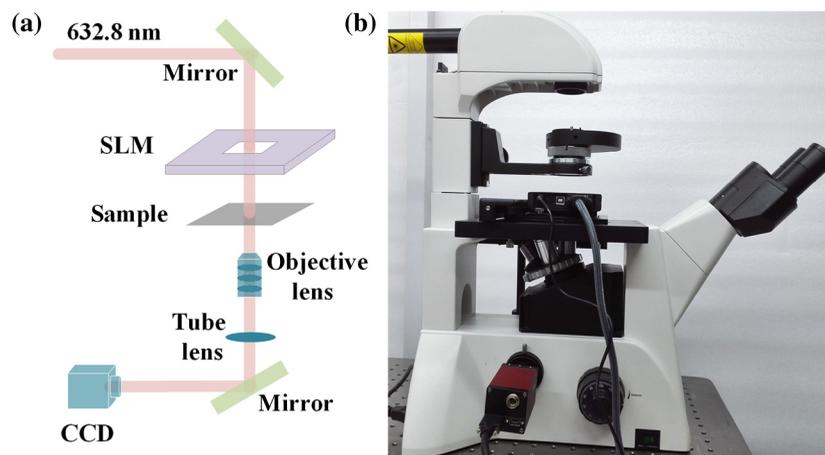

Fig. 3 (a) Schematic and (b) actual device of the ptychography-based microscope integrated with SLM.
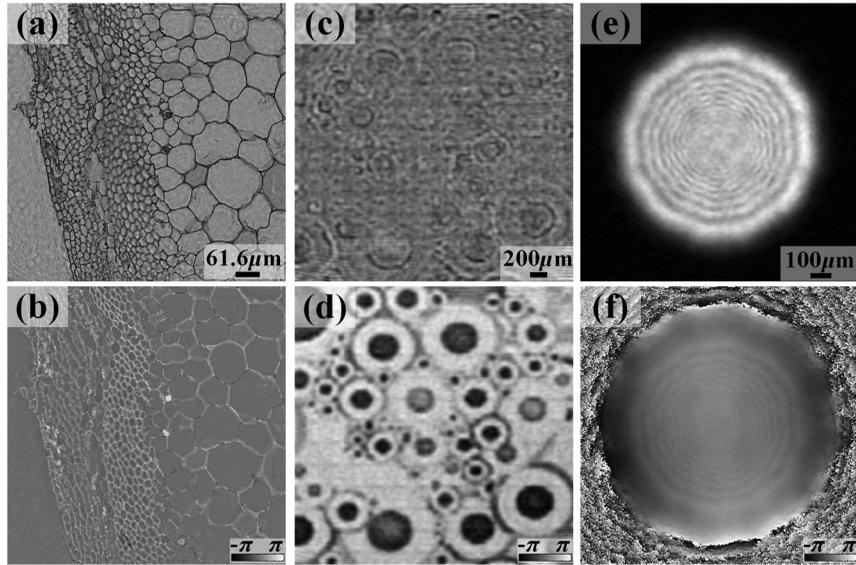
Fig. 4 Reconstructed (a) modulus and (b) phase of the sample; (c) modulus and (d) phase of the transmission distribution of the SLM; (e) modulus and (f) phase of the incident beam on the SLM.

that can be distinguished. For the imaging system demonstrated here, the theoretical resolution was calculated to be 2.53 μm. The achieved resolution of the ptychography-based microscope integrated with an SLM was also checked by measuring a US Air Force (USAF) 1951 resolution target, and the amplitude distribution obtained is shown in Fig. 5(c). In this imaging system, instead of the image of the sample, the magnified diffraction patterns were recorded by the CCD camera. The distance between the diffraction plane of the sample and the objective lens can be a little shorter than the standard working distance of the objective lens.[26] Accordingly, the resolution achieved is about 2.2 μm (the sixth element of group 8), which is a little higher than the theoretical value of 2.53 μm. In addition, the

reconstruction process converged very quickly according to the error curve shown in Fig. 5(d).

In the experiment described above, it took ∼2.8 s to acquire all of the 5 × 5 diffraction patterns. The overall acquisition speed of the experiment was mainly determined by the response time of the SLM, the data collection time of the CCD, and the data storage time of the computer. In the experiment mentioned above, the response time for a single picture displayed on the SLM at 632.8 nm was ∼16 ms, and the frame rate of the CCD camera was 27.8 fps when the exposure time was 6 ms. So, for 25 diffraction patterns, the response time of the SLM was ∼0.4 s, the data collection time of the CCD was ∼0.9 s, and data storage took 1.5 s. Because most of the time was spent on the data transfer from the CCD to the computer, the data acquisition time of our experiment could be further reduced by using a CCD with RAM. For the ptychography experiment using mechanical scanning, the data acquisition process involved scanning translation stages, the data collection time of the CCD, and the data storage time of the computer. The most time-consuming process was scanning, which involved acceleration, constant velocity movement, and deceleration. For most of the mechanical translation stages, the running speed was ∼1 mm/s, and the acceleration was ∼1.5 mm/s², which resulted in the time required for the mechanical stage to finish one step of scanning to be longer than 1 s. The response time of the SLM was usually much shorter than 30 ms. Thus, the SLM was at least 30 times faster than the mechanical scanning stage, which is definitely an advantage. In addition, when Galvo mirrors are used for ptychography, the response time can be comparable with that of an SLM in most cases, thus making the overall performance of Galvo mirrors no faster than an SLM. Moreover, the positioning error of the ptychography based on SLM is negligible when compared with that of Galvo mirrors.
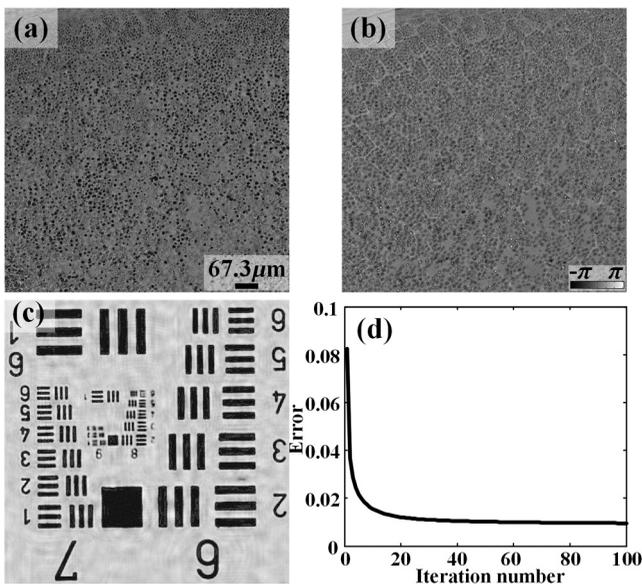
5 Conclusion

Although the proposed method of using an SLM to achieve ptychography is not practical in x-ray imaging, this method has several applications in the optical regime. It can not only be used to reform optical microscopes but also to measure

Fig. 5 Reconstructed (a) modulus and (b) phase distribution of a slice of corn seed; (c) amplitude distribution obtained for a USAF 1951 resolution target; and (d) progression of the error over 100 iterations.

dynamic physical phenomena, for example, the thermal recovery process of a crystal used in a high-power laser system or the deformation of a large optical element induced by its heavy weight. The method of ptychography has already been used to measure the thermal distortion in high-power laser glass elements.[27] However, the data acquisition speed of conventional ptychography cannot meet the temporal precision requirements of the thermal recovery process. Thus, the proposed method with a much faster acquisition speed is definitely an advantage in such cases.

Mechanical scanning of the sample relative to the illumination beam in conventional ptychographic techniques was replaced by displaying a moving picture on the SLM. This resulted in discovery of a robust solution to two major concerns in conventional ptychography—the long data acquisition time and position errors—that limit the scope of imaging in many applications. The acquisition time needed to collect 25 diffraction patterns using an SLM is ∼2.8 s, which is much faster than conventional ptychography based on mechanical scanning. The proposed method is highly beneficial in situations where the sample or the working environment cannot be kept stable for a sufficiently long time. This method has been successfully implemented in a commercial light microscope to achieve phase microscopy. The developed microscope has a simple structure, is insensitive to environmental disturbances, and can obtain speckle-free quantitative phase images, which would make it easy to adopt compared with other phase-contrast microscopy techniques.

Disclosures

Acknowledgments

References

1. S. Bradbury and P. J. Evennett, *Contrast Techniques in Light Microscopy*, Bios Scientific Publishers, Oxford, United Kingdom (1996).
2. M. Heilemann et al., "Photoswitches: key molecules for subdiffraction-resolution fluorescence imaging and molecular quantification," *Laser Photonics Rev.* **3**, 180–202 (2009).
3. G. Koopman et al., "Annexin V for flow cytometric detection of phosphatidylserine expression on B cells undergoing apoptosis," *Blood* **84**, 1415–1420 (1994).
4. G. E. Sommargren and B. J. Thompson, "Linear phase microscopy," *Appl. Opt.* **12**, 2130–2138 (1973).
5. P. Torok and F. J. Kao, *Optical Imaging and Microscopy*, Springer-Verlag, Germany (2003).
6. A. Barty et al., "Quantitative optical phase microscopy," *Opt. Lett.* **23**, 817–819 (1998).
7. J. B. Pawley, *Handbook of Biological Confocal Microscopy*, Plenum, New York (1995).
8. G. Popescu et al., "Fourier phase microscopy for investigation of biological structures and dynamics," *Opt. Lett.* **29**, 2503–2505 (2004).
9. C. G. Rylander et al., "Quantitative phase-contrast imaging of cells with phase-sensitive optical coherence microscopy," *Opt. Lett.* **29**, 1509–15011 (2004).
10. P. Marquet et al., "Digital holographic microscopy: a noninvasive contrast imaging technique allowing quantitative visualization of living cells with subwavelength axial accuracy," *Opt. Lett.* **30**, 468–470 (2005).
11. S. S. Kou et al. "Transport-of-intensity approach to differential interference contrast (TI-DIC) microscopy for quantitative phase imaging," *Opt. Lett.* **35**, 447–449 (2010).
12. A. M. Maiden, J. M. Rodenburg, and M. J. Humphry, "Optical ptychography: a practical implementation with useful resolution," *Opt. Lett.* **35**, 2585 (2010).
13. A. M. Maiden et al., "Superresolution imaging via ptychography," *J. Opt. Soc. Am. A* **28**, 604 (2011).
14. A. M. Maiden, M. J. Humphry, and J. M. Rodenburg, "Ptychographic transmission microscopy in three dimensions using a multi-slice approach," *J. Opt. Soc. Am. A* **29**, 1606 (2010).
15. T. M. Godden et al., "Ptychographic microscope for three-dimensional imaging," *Opt. Express* **22**, 12513 (2014).
16. J. Marrison et al., "Ptychography-a label free, high-contrast imaging technique for live cells using quantitative phase information," *Sci. Rep.* **3**, 2369 (2013).
17. L. Bian et al., "Fourier ptychographic reconstruction using Poisson maximum likelihood and truncated Wirtinger gradient," *Sci. Rep.* **6**, 27384 (2016).
18. X Ou et al., "Quantitative phase imaging via Fourier ptychographic microscopy," *Opt. Lett.* **38** 4845 (2013).
19. L. H. Yeh et al., "Experimental robustness of Fourier ptychography phase retrieval algorithms," *Opt. Express* **23**, 33214 (2015).
20. X. Ou, G. Zheng, and C. Yang, "Embedded pupil function recovery for Fourier ptychographic microscopy," *Opt. Express* **22**, 4960 (2014).
21. K. Guo, S. Dong, and G. Zheng, "Fourier ptychography for brightfield, phase, darkfield, reflective, multi-slice, and fluorescence imaging," *IEEE J. Sel. Top. Quantum Electron.* **22**, 6802712 (2016).
22. L. Tian et al., "Computational illumination for high-speed in vitro Fourier ptychographic microscopy," *Optica* **2**, 904 (2015).
23. L. Tian et al., "Multiplexed coded illumination for Fourier Ptychography with an LED array microscope," *Biomed. Opt. Express* **5**, 2376 (2014).
24. R. W. Gerchberg, "A practical algorithm for the determination of phase from image and diffraction plane pictures," *Optik* **35**, 237–246 (1972).
25. J. Fienup, "Phase retrieval algorithms: a comparison," *Appl. Opt.* **21**, 2758–2769 (1982).
26. T. M. Godden et al., "Ptychographic microscope for three-dimensional imaging," *Opt. Express* **22**, 12513–12523 (2014).
27. H. Wang et al., "Measurement of thermal distortion in high power laser glass elements using ptychography," *Laser Phys. Lett.* **12**, 025005 (2015).

Yudong Yao is currently a PhD student in optical engineering at Shanghai Institute of Optics and Fine Mechanics, Chinese Academy of Sciences, under the supervision of professor Jianqiang Zhu and professor Cheng Liu. Her research focuses on the development and application of phase retrieval methods.

Biographies for the other authors are not available.